Intramedullary Mg2Ag nails augment callus formation during fracture healing in mice

Katharina Jähn [a,b,c,1], Hiroaki Saito [b,c,1], Hanna Taipaleenmäki [b,c], Andreas Gasser [b,c], Norbert Hort [a,d], Frank Feyerabend [a,d], Hartmut Schlüter [a,e], Johannes M. Rueger [a,c], Wolfgang Lehmann [a,c], Regine Willumeit-Römer [a,d], Eric Hesse [a,b,c,f,*]

[a] Helmholtz Virtual Institute for Magnesium-based Bio-degradable Materials, Germany

[b] Heisenberg-Group for Molecular Skeletal Biology, University Medical Center Hamburg-Eppendorf, Hamburg, Germany

[c] Department of Trauma, Hand and Reconstructive Surgery, University Medical Center Hamburg-Eppendorf, Hamburg, Germany

[d] Institute of Materials Research, Helmholtz-Center Geesthacht, Geesthacht, Germany

[e] Institute of Clinical Chemistry and Laboratory Medicine, University Medical Center Hamburg-Eppendorf, Hamburg, Germany

[f] Department of Anatomy and Cell Biology, Indiana University School of Medicine, Indianapolis, USA

[*] Corresponding author. Heisenberg-Group for Molecular Skeletal Biology, Department of Trauma, Hand and Reconstructive Surgery, University Medical Center Hamburg-Eppendorf, Research Campus N27, Martinistrasse 52, D-20256 Hamburg, Germany. Tel.: +49-40-7410-54114; fax: +49-40-7410-40196; email: e.hesse@uke.de.

[1] These two authors contributed equally.

This is the author's manuscript of the article published in final edited form as:
Jähn, K., Saito, H., Taipaleenmäki, H., Gasser, A., Hort, N., Feyerabend, F., … Hesse, E. (2016). Intramedullary Mg2Ag nails augment callus formation during fracture healing in mice. Acta Biomaterialia, 36, 350–360.
http://doi.org/10.1016/j.actbio.2016.03.041

Abstract

Intramedullary stabilization is frequently used to treat long bone fractures. Implants usually remain unless complications arise. Since implant removal can become technically very challenging with the potential to cause further tissue damage, biodegradable materials are emerging as alternative options. Magnesium (Mg)-based biodegradable implants have a controllable degradation rate and good tissue compatibility, which makes them attractive for musculoskeletal research. Here we report for the first time the implantation of intramedullary nails made of an Mg alloy containing 2% silver (Mg2Ag) into intact and fractured femora of mice. Prior *in vitro* analyses revealed an inhibitory effect of Mg2Ag degradation products on osteoclast differentiation and function with no impair of osteoblast function. *In vivo*, Mg2Ag implants degraded under non-fracture and fracture conditions within 210 days and 133 days, respectively. During fracture repair, osteoblast function and subsequent bone formation were enhanced, while osteoclast activity and bone resorption were decreased, leading to an augmented callus formation. We observed a widening of the femoral shaft under steady state and regenerating conditions, which was at least in part due to an uncoupled bone remodeling. However, Mg2Ag implants did not cause any systemic adverse effects. These data suggest that Mg2Ag implants might be promising for intramedullary fixation of long bone fractures, a novel concept that has to be further investigated in future studies.

Keywords: Mg2Ag alloy, Biodegradation, Intramedullary fracture fixation, Bone healing, Callus formation

1. Introduction

Fractures of the femoral and tibia shaft often occur in response to high energy trauma and are preferentially treated by an intramedullary nail that supports the fracture zone and facilitates bone healing [1–3]. The intramedullary stabilization usually remains since implant removal in general and extraction of a nail in particular can be very time-consuming, cumbersome and may cause further tissue damage, re-fracture and other subsequent problems [4–6]. Thus, the second surgery imposes a potential risk to the patient and causes additional costs. However, pain, dysesthesia, a broken nail, infection, pseudarthrosis or the need for implanting a hip or knee prosthesis later in life may require removal of the intramedullary nail [5,6]. Thus, biodegradable implants represent an attractive alternative to replace conventional implants. Among the various biodegradable materials, magnesium (Mg) and Mg-containing alloys have a long history in the musculoskeletal field [7]. Based on their high biocompatibility, biodegradability, and similar mechanical properties to bone, many studies investigated the use of Mg and its alloys for applications in orthopedic surgery [8–17]. In addition to its favorable mechanical properties, Mg has been shown to increase osteoblast differentiation *in vitro* [18,19] and to induce new bone formation *in vivo* [13], demonstrating a high osteogenic potential. Furthermore, as screws for hallux valgus surgery, Mg-based implants are already in use for clinical applications [10,20]. However, these implants are much smaller than intramedullary nails and are not entirely surrounded by bone marrow, an environment that might affect implant degradation and tissue response.

Among the challenges with Mg implants are the degradation rate and the biocompatibility [13–15]. For instance, Mg-Calcium alloys are biocompatible but degrade quite rapidly [21,22]. Mg-Fluoride coating has been reported to reduce the *in vivo* degradation rate of Mg implants and rare earth metals that are frequently used

as alloy materials for Mg can cause cytotoxic effects [23,24]. Recently, members of our consortium reported a novel Mg alloy containing 2% silver (Mg2Ag), which was cast and treated by a solidification cooling process, resulting in appropriate mechanical properties and a rather low degradation rate. Furthermore, *in vitro* investigations of this alloy showed favorable antibacterial effects and no cytotoxicity to human osteoblasts [25].

To investigate the *in vivo* degradation of this novel material as well as its impact on bone remodeling and fracture healing, we implanted Mg2Ag intramedullary nails into mice with and without a femoral shaft fracture, followed by an analysis of *in vivo* degradation and tissue response under steady-state and bone healing conditions. Degradation of Mg2Ag alloys *in vivo* occurred without adverse effects but faster than *in vitro*. Mice were overall healthy and no adverse effects on body weight or kidney, liver, muscle, or spleen were observed. Radiographs and bone histomorphometry revealed that in comparison to steel implants, fractures supported by Mg2Ag intramedullary nails demonstrated a decreased bone resorption while bone formation was increased, leading to a significantly bigger callus during the first 21 days of fracture healing. These results demonstrate that fixation of long bone shaft fractures by intramedullary Mg2Ag nails might be a promising concept for further investigation.

2. Materials and methods

2.1. Mg2Ag implant preparation

Production of the Mg2Ag (2% Ag, wt/wt) alloy was performed by permanent mold casting using pure (99.99%) Mg and pure (99.99%) Ag granules. Briefly, molten Mg was maintained at 720°C and pre-heated Ag (150°C) was added under continuous stirring (200 rpm) for 15 min. The melt was poured into a mild steel mold pre-heated to 550°C. For better separation of castings from the mold, hexagonal boron nitride

was used as mold release agent. In one casting, 6 ingots with a diameter of 30 mm and a length of >170 mm were produced. During the casting process cover gas (Ar + 0.5% SF_6) was applied. Ingots were cut to a length of 80 mm and trimmed to a diameter of 28 mm. Next, the alloy was homogenized in Ar (6 h at 420°C), followed by an extrusion at 370°C with an extrusion ratio of 1/16 from a diameter of 28 mm to 3 mm. The extrusion speed was 4.5 mm/s. For wire production, the extruded rods were cut to 90 mm length and drawn by hand from a diameter of 3 mm to the final diameter of 0.8 mm in 0.05 mm increments. Prior to each drawing step, wires were heated to 300°C for 45 min until a diameter of 1.6 mm was reached. At smaller diameters the heating time was reduced to 15 min. Standard drawing dies, pliers, and draw wax as lubricant were used on a drawing bench.

2.2. Implant characterization

Composition of the alloy was determined by energy-dispersive X-ray spectroscopy analysis (XRF) (Bruker Explorer S4, Bruker AXS GmbH, Karlsruhe, Germany).

2.3. In vitro degradation of Mg2Ag implants and quantification of osmolality and pH

Mg2Ag wires of a diameter of 0.8 mm and a length of 20 mm were incubated in 3 ml DMEM containing 10% fetal bovine serum (FBS) at cell culture conditions (37°C, 5% CO_2, 95% humidity). Initial weight was determined and compared to the weight after 7 days of incubation. The average *in vitro* degradation rate was calculated using the weight differences of 6 independent samples. During the 7 days of incubation, changes in pH and osmolality of the supernatant were determined using a pH meter and a Gonotec 030D cryoscopic osmometer (Gonotec, Berlin, Germany), respectively.

2.4. Preparation of medium conditioned with Mg2Ag implant degradation products

Mg2Ag degradation products were prepared as described previously [26]. Briefly, Mg2Ag disks of 1 cm in diameter were immersed for 24 h in α-MEM containing 10% FBS and maintained under cell culture conditions (37℃, 5% CO_2, 95% humidity). Conditioned medium (CM) enriched with Mg2Ag degradation products was added to osteoblast and osteoclast cultures at a final concentration of 20%, 10% or 3.3%. Mg concentration in the CM was determined by the xylidylblue-I chromogenic method according to the manufacturers instructions (Mg Assay Kit, Biomol GmbH, Hamburg, Germany). The effect of the CM on cell differentiation and function was compared to normal differentiation medium as control.

2.5. Osteoblast and osteoclast cultures

Long bone osteoblasts and bone marrow-derived osteoclast precursors were isolated from ten-week old C57Bl/6J wild type mice according to standard protocols [27,28]. Briefly, tibiae and femora were harvested and cleaned with a forceps and scalpel to remove adjacent soft tissues. Epiphyses were cut and bone marrow was flushed to obtain osteoclast precursor cells. Cells were then seeded into 10 cm² dishes with α-MEM containing 10% FBS and 1% Penicillin/Streptomycin (P/S). After incubation for 3 h, non-adherent osteoclast precursors were transferred into a new 10 cm² dish and cultured in α-MEM supplemented with 10% FBS and 1% P/S for 2 days in the presence of 100 ng/ml macrophage colony stimulating factor (M-CSF, PeproTech, INC, Rocky Hill, NJ, USA). Next, osteoclast precursors were transferred into 96-well plates at a density of 45.000 cells/cm^2 and were cultured in α-MEM with 10% FBS and 1% P/S containing 25 ng/ml M-CSF and 100 ng/ml recombinant human receptor activator of NF-κB Ligand (RANKL, PeproTech, INC, Rocky Hill, NJ, USA). Mature, multinucleated osteoclasts formed after 4 days in culture and were

visualized by staining for tartrate resistant acid phosphatase (TRAP) activity. TRAP activity was detected in osteoclasts fixed by 4% neutral buffered formalin. For the staining, a sodium acetate buffer containing sodium tartrate (pH=5) and naphthol-ASMX-phosphate as well as fast red violet as substrates was used. The number and the size of the osteoclasts were quantified using the Osteomeasure system (OsteoMetrics, Decatur, GA, USA). Pit formation, a measure of osteoclast function, was determined by seeding 45.000 osteoclast precursors/cm^2 into 96-well plates containing dentin slices. Cells were differentiated in α-MEM containing 10% FBS, 1% P/S, 25 ng/ml M-CSF and 100 ng/ml RANKL. After 6 days of differentiation, cells were removed from dentin slices by incubation in 20% bleach for 5 min. Resorption pits were stained with 1% toluidine blue at pH 4.5. The area and the number of resorption pits were quantified using the Osteomeasure system.

Long bone envelopes remaining after flushing of the bone marrow were used for osteoblast outgrow cultures. Briefly, bones were cut into 1-2 mm^2 pieces and digested in 1 ml α-MEM containing 2 mg/ml collagenase A (Roche Diagnostics, Indianapolis, IN, USA) for 2 h at 37°C for fibroblast removal. Bone pieces were then placed in α-MEM supplemented with 10% FBS and 1% P/S for 7 days to allow osteoblasts to outgrow onto tissue culture plastic. Next, osteoblasts were seeded at a density of 10.000 cells/cm^2 into 96-well plates. Osteoblasts were then differentiated in the presence of 50 µg/mL L-ascorbic acid (Sigma Aldrich, St. Louis, MO, USA) and 5 mM β-glycerol phosphate (EMD Millipore Corp., Billerica, MA, USA). Next, CM was added at a relative concentration of 3.3%, 10% or 20%. Non-supplemented culture medium served as control. Medium was changed every 2 days. Osteoblast differentiation was determined by staining of alkaline phosphatase (ALP) activity on day 7. For this purpose, cells were fixed with 4% neutral buffered formalin and stained in Tris-HCl buffer containing naphthol AS-MX and fast blue at 37°C.

2.6. Implantation of Mg2Ag pins and femoral fractures

All animal work was conducted at the University Medical Center Hamburg-Eppendorf according to the German law after approval by the local authorities (animal protocol number: 102/14). Ten-week old male C57Bl/6J wild type mice were used for *in vivo* studies. To determine the *in vivo* degradation of Mg2Ag implants, we implanted Mg2Ag pins into the non-fractured right femur of mice. These mice were compared to mice that received a steel implant or no implant as controls. All implants were inserted into the right femur in a minimally invasive manner after skin excision over the knee joint and perforation of the cortical bone at the inter-condylar notch using a 21-gauge needle. The implants had a diameter of 0.8 mm and were cut to a length that allowed the implant to be located fully underneath the surface of the articular cartilage. The skin was closed using a surgical suture. Mice were placed on a warm pad with access to pain relieve medication while recovering from anesthesia. Animals were examined by day 30, 60 and 210 after implantation with 4 mice per group and time point.

In order to investigate the degradation of Mg2Ag pins under fracture repair conditions and to determine the effects of the implants on bone remodeling during bone healing, a model of an open femoral shaft fracture was used. Briefly, animals were anesthetized using a combination of ketamine (120 mg/kg body weight) and xylazine in saline (16 mg/kg body weight). At the lateral side of the right femur, an incision of 8 mm length was placed along the femoral shaft and muscles were gently pushed aside to expose the femur. Next, an incision was placed over the right knee joint and the cortical bone was perforated at the inter-condylar notch using a 21-gauge needle, followed by the insertion of a Mg2Ag or steel pin into the distal femur. The femur was then fractured in the mid-shaft region using a bone cutter. Implants

were moved forward over the fracture into the proximal femur. Skin incisions were then sutured. Animals were recovered from anesthesia on a warm pad with access to pain relieve medication. Mice were injected with calcein and demeclocycline (each at 40 mg/kg body weight) 5 days and 2 days prior to sacrifice, respectively, to label active surfaces of bone formation as a surrogate of osteoblast activity. By day 7, 14, 21 and 133 after fracture, mice were analyzed with 6 to 11 animals per group and time point.

2.7. X-ray and micro-computed tomography

Degradation of the Mg2Ag implants and fracture healing were followed by X-ray imaging with life animals under anesthesia at the indicated time points using a X-ray imager (Faxitron Xray corporation, Tucson, USA). Images were obtained at 36 kV with 4 s exposure time.

Micro-computed tomography (µCT) imaging was performed as a more sensitive approach to determine implant degradation and fracture healing. Briefly, femora were harvested and fixed in 4% neutrally buffered formalin for 48 h prior to storage in 70% ethanol. Scans were obtained using a Scanco VivaCT 80 scanner (Scanco Medical AG, Brüttisellen, Switzerland) at 70 kV, 114 µA, 16.5 µm/voxel resolution, 400 ms integration time and a threshold of 326 mg HA/ccm. Three-dimensional images were reconstructed using Imaris software 8.0 (Bitplane, Concord, MA, USA).

2.8. Histological analysis

At the indicated time points of analysis, femora and several organs including liver, spleen, kidney, and rectus femoris muscle adjacent to the surgical site were harvested. All samples were fixed in 4% neutral buffered formalin for 48 h. Soft

tissues were dehydrated and embedded in paraffin. Sections of 5 µm thickness were prepared and stained with haematoxylin and eosin.

Bones were prepared for histology as described previously [29]. Briefly, bones were cleaned from surrounding soft tissue and steel implants were removed. Next, bones were dehydrated to absolute ethanol, followed by infiltration and embedding in methyl methacrylate. Longitudinal sections of 5 µm thickness were prepared at the central plane and stained by von Kossa/van Gieson, Toluidine blue, Masson Goldner trichrome, or mounted unstained. Histomorphometry of bone sections was performed using ImageJ and the Osteomeasure system. The particle analysis function of ImageJ was applied to determine the amount of bone in the callus using von Kossa/van Gieson-stained sections. For all other quantifications, the Osteomeasure system was used according to ASBMR guidelines where applicable [30]. Toluidine blue-stained sections were used to quantify the callus area and the amount of cartilage within the callus. Furthermore, Toluidine blue and Masson Goldner-stained sections were used to determine cellular parameters at the periosteal elevation site of the callus. In addition, unstained sections were subjected to dynamic histomorphometry to quantify bone formation rates at the periosteal elevation site of the callus.

2.9. Statistics

IBM SPSS statistics software 21 was used for statistical analysis. Student's t-test was applied to compare two independent experimental groups. Multiple groups were analyzed by one-way ANOVA with Tukey's post-hoc test. For all statistical comparisons, p-values ≤ 0.05 were considered statistically significant.

3. Results

3.1. Alloy composition and *in vitro* degradation

3.1.1. Analysis of Mg2Ag implants

Implant characterization by XRF revealed a content of 1.94 ± 0.05% (wt/wt) Ag. Impurities due to the natural composition of Mg, Ag and the alloying process were minor with 22.3 ± 2.4 ppm Fe, 20 ± 2.2 ppm Cu, 14.5 ± 1.1 ppm Ni, and 0.43 ± 0.03 ppm Be.

3.1.2. *In vitro* degradation, osmolality and pH

In vitro degradation of Mg2Ag implants was investigated during a time course of 7 days. The surface of the implant was smooth by day 0 (Fig. 1a, upper panel) and became rough within 7 days (Fig. 1b, lower panel). The corrosion rate was determined as 0.473 ± 0.038 mm/year. During the 7 days of degradation, the osmolality of the medium increased only very modestly from 0.328 osmol/kg to 0.359 ± 0.003 osmol/kg, without reaching statistical significance (Fig. 1b). No significant changes in pH were detected, which remained stable during the course of the experiment (Fig. 1c).

3.2. Effect of degradation products on bone cell differentiation and function

3.2.1. Osteoblast differentiation

To determine the effect of Mg2Ag implant degradation products on osteoblast differentiation, mouse long bone osteoblasts were cultured with 3.3%, 10% and 20% medium conditioned with Mg2Ag implant degradation products, which corresponds to Mg concentrations of 0.22 mg/ml, 0.64 mg/ml and 1.28 mg/ml. Analysis of osteoblast

differentiation was determined after 7 days in culture by staining for ALP activity. The increasing amount of CM did not affect ALP activity, demonstrating that Mg2Ag degradation products had no influence on osteoblast differentiation *in vitro* (Fig. 1d).

3.2.2. Osteoclast differentiation and function

Differentiation of murine osteoclast precursors into mature osteoclasts was investigated by quantifying the number and the size of tartrate-resistant acid phosphatase (TRAP)-positive cells that had more than three nuclei. These assays revealed that the numbers of TRAP-positive multinucleated osteoclasts as well as the size of these cells were reduced by an increasing amount of CM (Fig. 1e, f). Furthermore, osteoclast function was determined by dentin resorption assays. Quantification of the area and the number of the pits revealed an antagonistic effect of the CM at higher concentration (Fig. 1g, h). These findings provide strong evidence that Mg2Ag degradation products inhibit osteoclast differentiation and function *in vitro*.

3.3. Degradation of Mg2Ag implants *in vivo*

3.3.1. Analysis of side effects

To determine if Mg2Ag implants cause adverse effects *in vivo*, Mg2Ag and steel pins were implanted into the right femur of mice. Compared to age matched mice that had no implant, mice that were implanted with Mg2Ag or steel pins did not show any abnormal activity or behavior (data not shown), or any difference in body weight over a period of 210 days (Fig. 2a). Various organs including liver, spleen, kidney and muscle were harvested for histological analysis 30 and 210 days after implantation. Consistent with the overall well being of all animals, no histological abnormalities

were observed in these organs of mice implanted with Mg2Ag pins compared to mice that received a steel pin or no implant (Fig. 2b). Taken together, these data indicate that the implantation of Mg2Ag pins into the medullary canal of the right femur does not cause measurable side effects on the growth rate or on inner organs morphology.

3.3.2. Implant degradation *in vivo*

Next we sought to investigate the *in vivo* degradation of Mg2Ag pins after implantation into non-fractured femora of mice using X-ray and µCT analysis. Imaging by X-ray was performed immediately after surgery to confirm the correct positioning of the implant and after 30, 60 and 210 days to follow implant degradation. While all implants remained in their initial position without signs of loosening or displacement, a considerable degradation of Mg2Ag implants was appreciated 210 days after implantation (Fig. 3a). These data were then confirmed and further investigated by a higher resolution *ex vivo* µCT analysis 30, 60 and 210 days after insertion of the implant. Degradation of the Mg2Ag implant was detectable already by day 30, continued by day 60 (Fig. 3b) and was almost completed by day 210 (Fig. 3b, c). Interestingly, while the almost complete degradation of a Mg2Ag pin of 0.8 mm implanted into the medullary canal of a mouse femur takes approximately 210 days, the time for the same implant to degrade *in vitro* was predicted to be 617 days (see 3.1.2.) and therefore almost three times longer. We also noted that femora of animals of the Mg2Ag group appeared to have a widening of the femoral shaft compared to mice that received an intramedullary steel pin or no implant (Fig. 3b, c). To further investigate this interesting observation, femoral diameters at the midshaft were measured by µCT analysis. Indeed, intramedullary Mg2Ag pins significantly increased the femoral diameter compared to both control groups by about 40% (Fig. 3c).

3.4. Effect of intramedullary Mg2Ag implants on fracture healing

3.4.1. Exclusion of systemic adverse effects

First we wanted to test the hypothesis that Mg2Ag implants do not cause side effects during fracture healing. We therefore analyzed the body weight and the microscopic structure of liver, spleen, kidney and muscle obtained from mice that received a fracture fixation using an intramedullary Mg2Ag pin compared to control animals in which the fracture was stabilized by a steel implant. Quantification of the body weight showed an age-related increase 133 days after fracture without difference between groups, suggesting that intramedullary Mg2Ag implants do not affect animal growth under fracture conditions (Fig. 4a). This notion was further confirmed by histological analysis of various organs including liver, spleen, kidney and muscle at post-fracture day 7 and 133, which showed no histological abnormality of any organ of mice implanted with a Mg2Ag pin (Fig. 4b). These data confirm, that like under non-fracture conditions, intramedullary Mg2Ag pins do not cause acute or long-term systemic adverse effects.

3.4.2. Imaging of implant position, degradation and fracture healing

Confirmation of the correct position of the intramedullary implant was performed by X-ray analysis immediately after implantation and on day 14, 21 and 133 (Fig. 5a). Using the same technique, mice were followed for up to 133 days after fracture, demonstrating the formation and remodeling of the callus in both groups and the degradation of the Mg2Ag implant during the course of the experiment (Fig. 5a). Next, we applied *ex vivo* µCT imaging as a method of higher sensitivity and resolution and found that the callus was fully developed already by day 14 in mice in

which the fracture was stabilized by a Mg2Ag pin, a time point at which callus formation just started to begin in the control group (Fig. 5b). Furthermore, callus formation was considerably stronger in response to Mg2Ag implants by day 21 while a complete fracture healing was observed in both groups (Fig. 5b). Interestingly, µCT imaging revealed an increase of the femoral midshaft diameter of 73 ± 6% in animals implanted with Mg2Ag pins compared to control animals at day 133 (Fig. 5c), suggesting that bone remodeling might be affected by Mg2Ag implants during fracture healing compared to steel pins. This increase in diameter of the femoral midshaft is consistent with the observation of a widening of the femoral shaft in response to Mg2Ag implants in non-fractured mice (Fig. 3c). However, the relative increase in diameter is greater in fractured compared to non-fractured bones. This indicates that intramedullary Mg2Ag implants might affect bone remodeling by influencing the activity of osteoclasts and osteoblasts and that this effect is augmented in the context of an activated bone remodeling during fracture healing.

3.4.3. Analysis of callus formation, cartilage turnover and mineralization

Consistent with the finding made by µCT, histological analysis of mineralized tissue by day 14 and 21 after fracture confirmed the formation of a callus that was normally mineralized but augmented in mice, in which the long bone fracture had been stabilized by an intramedullary Mg2Ag implant compared to control animals (Fig. 6a). In both groups, fracture healing was completed successfully with a full removal of the callus by day 133 (Fig. 6a). To further characterize the influence of Mg2Ag implants on fracture repair, bones were investigated at early time points during fracture healing by dedicated histomorphometry. Fracture stabilization using a steel implant led to a significant increase in callus size between day 7 and day 14, followed by a decrease of the callus size between day 14 and day 21 (Fig. 6b). In

contrast, Mg2Ag implants led to a callus that was significantly larger compared to the control group as early as day 7 and at all subsequent points of analysis. Furthermore, the size of the callus did not decrease 14 days after fracture, demonstrating an augmented callus formation due to intramedullary Mg2Ag implants (Fig. 6b).

Fracture repair resembles endochondral ossification, a process during which cartilage tissue is formed and subsequently replaced by mineralized bone. To determine abnormalities in endochondral ossification in response to Mg2Ag implants, we quantified both the relative amount of cartilage and the relative amount of mineralized bone within the callus. In both groups, the amount of cartilage per callus was around 50% by day 7 and decreased during the following 2 weeks of fracture repair without major differences except for a greater decrease in cartilage by day 21 in the group of mice that received Mg2Ag implants, suggesting a slightly increased turnover rate (Fig. 6c). Indicating an accelerated mineralization, by day 7 the relative amount of mineralized bone within the callus was significantly higher in mice in which fractures were stabilized by Mg2Ag implants compared to control animals (Fig. 6d). By day 14 and day 21, the amount of mineralized bone within the callus was significantly increased compared to day 7 with no differences among groups (Fig. 6d). In summary, these data suggest that intramedullary Mg2Ag implants augment callus formation with an accelerated mineralization at the beginning of the fracture healing and an increased cartilage turnover towards the end of the remodeling phase.

3.4.4. Quantification of bone formation and bone resorption

Next we sought to determine osteoblast activity on trabeculae of the fracture callus and at the periosteal elevation site after labeling of bone surfaces with calcein and demeclocycline at a defined time interval. Compared to fractures that were stabilized

with steel implants, the distance between the labels was greatly increased at the periosteal elevation site 21 days after fracture fixation using Mg2Ag pins and the newly produced bone matrix appeared as less organized woven bone, suggesting a highly activated osteoblast activity (Fig. 7a). Indeed, the mineral apposition rate (MAR), a parameter calculated from the distance of the labeled bone surfaces, was significantly increased in response to fracture stabilization by Mg2Ag implants compared to steel control pins at all time points investigated during 21 days of fracture healing (Fig. 7b). Analysis of bone formation on trabecular bone surfaces within the callus by day 21 after fracture also revealed an increased distance between fluorescent labels (Fig. 7c), representing a significantly increased bone formation rate per bone surface in response to Mg2Ag implants compared to control animals receiving steel implants (Fig. 7d). These data demonstrate that intramedullary Mg2Ag implants activate bone formation, leading to an increased callus formation.

Since Mg2Ag implants accelerated the mineralization of the newly formed callus at early stages (Fig. 6d), we speculated that despite the increased bone formation rate the amount of osteoid per bone surface might be unchanged, due to the rapid mineralization of the new matrix. Indeed, there was no difference in the amount of osteoid between both groups (Fig. 7e), demonstrating the fast incorporation of minerals into the matrix in response to Mg2Ag implants. Furthermore, the number of osteoblasts was unaffected by Mg2Ag pins compared to control (Fig. 7f), further supporting the notion of an increased rate of bone-matrix production that undergoes rapid mineralization.

Bone resorption is an integral component of bone remodeling during fracture repair. Since *in vitro* analyses revealed that Mg2Ag degradation products inhibited osteoclast differentiation and function (Fig. 1e-f), we hypothesized that bone

resorption could be compromised *in vivo* during fracture healing in response to intramedullary Mg2Ag implants. To address this question we quantified the amount of eroded surface per bone surface and determined the number of osteoclasts per bone surface. Consistent with the *in vitro* findings, we observed that intramedullary Mg2Ag implants significantly decreased both bone resorption (Fig. 7g) reflecting osteoclast activity and the number of osteoclasts (Fig 7h). The reduction in bone resorption therefore contributes to the augmented callus formation by intramedullary Mg2Ag implants during fracture healing in mice.

4. Discussion

Intramedullary nailing is frequently used to stabilize long bone fractures [2]. After fracture healing, the nail usually remains but under certain circumstances such as pain or the need for another implant, removal of the intramedullary nail might become necessary [4,5]. Thus, biodegradable materials, including Mg-alloys, are promising alternatives that could obviate the need for implant removal [8,9,13,20]. Although Mg-based implants have a long history in musculoskeletal research [7], degradation, biocompatibility and the influence on bone tissue of intramedullary Mg2Ag nails under steady state and fracture conditions has not yet been investigated. To address these questions, we used intact, i.e. non-fractured, mouse femora and an open midshaft bi-cortical femoral fracture model in mice. Prior to analyzing this *in vivo* system, we performed *in vitro* experiments to determine the degradation of the Mg2Ag alloy, which was calculated to require about 1.7 years for the implant to fully degrade without affecting the osmolality or the pH of the environment. Compared to other Mg-based alloys, this degradation rate is rather slow and favorable for a potential use as bone implants [21,22]. As a prerequisite for bone implants, the Mg2Ag alloy should not cause any effects on bone cells that could compromise

fracture healing. We therefore investigated the influence of medium enriched with products resulting from the degradation of Mg2Ag on osteoblasts and osteoclasts. Our results demonstrate that osteoblast differentiation was unaffected by medium containing Mg2Ag degradation products, while osteoclast differentiation and function was greatly inhibited in a dose-dependent manner. These findings are consistent with those reported by others and are in support of further investigating this novel material in musculoskeletal research [25,26,31].

Next, we implanted custom-made intramedullary Mg2Ag nails of 0.8 mm diameter into non-fractured femora of adult mice. Imaging analysis using x-ray and µCT revealed that the implants were almost entirely degraded after 210 days, which is about three times faster than the degradation rate determined *in vitro*. Discrepancies between *in vitro* and *in vivo* degradation rates have been reported previously and emphasize the importance of *in vivo* degradation studies since a plethora of environmental cues including cell-based influences of the bone marrow environment, mechanical stimulation or continuous exchange of the liquids surrounding the implant may affect the degradation of the implant [32]. Nevertheless, the *in vivo* degradation of Mg2Ag intramedullary nails reported here occurs at a rate that provides sufficient mechanical stability while supporting fracture healing.

Neither under non-fracture nor under fracture conditions systemic adverse effects caused by Mg2Ag implants were observed based on a stable body weight of the experimental animals and a normal histological appearance of various inner organs at different time points. Consistent with our observations, others reported that the implantation of a Mg-Y-Zn alloy into pigs did not result in any systemic side effects, demonstrating high biocompatibility of the material [33]. In addition, implantation of a Mg-Y-Nd alloy containing heavy rare-earth elements into rats showed no systemic inflammatory reactions in blood smears of operated animals [34]. Thus, the findings

reported by others and the results shown here support the notion that Mg-based implants do not cause deleterious effects on animal growth or on inner organs.

Dedicated histomorphometric analysis of fracture healing revealed an increase in osteoblast activity, which led to an augmented bone formation rate and subsequent enhanced callus production. Early mineralization of the callus was enhanced and then continued normally. Furthermore, the Mg2Ag alloy reduced the number and activity of osteoclasts, a finding that is consistent with our *in vitro* observations and with the results reported by others [26,31,35]. Thus, the increased callus formation mediated by intramedullary Mg2Ag implants during fracture healing in mice is probably due to both an increase in bone formation and a decrease in bone resorption. These findings therefore strongly suggest the suitability of degradable Mg2Ag implants to promote long bone fracture healing in mice and are consistent with studies reporting positive effects of Mg implants on osteoblasts and bone formation [12–14,31,36,37]. However, we also noticed that Mg2Ag implants caused alterations of the shape of long bones under non-fracture and fracture conditions. Mg2Ag nails induced a widening of the femoral shaft without an obvious effect on the thickness of the cortical bone. We assume that these changes in bone shape are, at least in part, a consequence of the disturbed bone remodeling with an enhanced bone formation and an attenuated bone resorption, leading to an unbalanced turnover of the entire bone. Nevertheless, these findings require continued investigations in subsequent studies to further determine the suitability of biodegradable Mg2Ag alloys as material for intramedullary nails to treat long bone fractures.

5. Conclusions

Our study demonstrates that Mg2Ag-based intramedullary nails are suitable implants for the fixation of femoral fractures in mice. The material stimulated bone formation while inhibiting bone resorption, leading to an augmented callus formation during fracture healing. Mg2Ag implants degraded within a reasonable period of time without causing systemic adverse effects. Thus, Mg2Ag might be a promising material to be further investigated for potential applications in musculoskeletal medicine.

Disclosures

The authors declare that none of them have any conflicts of interest related to the content of this article.

Acknowledgements

The authors would like to thank Dr. Tie Di for wire drawing, Günter Meister for casting the alloy, Gabor Szakacs for casting and extrusion of the alloy, Sabine Schubert for chemical analyses and Gert Wiese for metallography (all Helmholtz Center Geestacht). We are grateful to Felix Gensch (Technical University Berlin) for supporting alloy extrusion and to Diana Zarecneva (University Medical Center Hamburg-Eppendorf) for help with soft tissue histology. This work was funded by the Helmholtz Gemeinschaft (VH-VI-523) and in part by the Deutsche Forschungsgemeinschaft (HE 5208/2-1).

Figure Legends

Fig. 1. (a) Surface analysis of Mg2Ag implant prior to degradation (day 0, upper panel) and during degradation (day 7, lower panel) in cell culture medium (scale bar = 0.8 mm). Change of osmolality (b) and pH (c) of the medium during degradation. Graphs show mean values ± SEM, n = 6. Analysis of osteoblast and osteoclast differentiation in the presence of conditioned medium (CM) containing an increasing concentration of Mg2Ag degradation products. (d) Alkaline phosphatase staining of osteoblasts on day 7 (scale bar = 100 µm). (e) Tartrate-resistant acid phosphatase (TRAP) staining of osteoclasts on day 4 (scale bar = 100 µm), blue arrows: mono-nucleated TRAP-positive osteoclast precursors, black arrows: multi-nucleated TRAP-positive mature osteoclasts. (f) Quantification of the number and the size of osteoclasts. (g) Resorption pits on dentin 6 days after plating of osteoclast precursors (scale bar = 50 µm). (h) Quantification of the area and the number of the resorption pits. (d, e, g) Representative images of 4 independent experiments. (f, h) Graphs show mean ± SEM, n = 9 samples per group, * = $p \leq 0.05$, ** = $p \leq 0.001$, significant compared to the groups that were treated with control medium.

Fig. 2. (a) Quantification of body weight of mice after implantation of Mg2Ag pins compared to mice receiving a steel implant or no implant as control. Graph shows mean values ± SEM, n = 4 animals per group. (b) Representative images of hematoxylin & eosin-stained sections of liver, spleen, kidney and muscle at day 30 and day 210 after implantation of a Mg2Ag pin compared to mice that received a steel pin or no implant as control, 20x magnification (scale bar = 100 µm), small boxes = area of digital magnification, large boxes: 13.5x digital zoom.

Fig. 3. Bone morphology and implant degradation of mice implanted with Mg2Ag pins without fracture compared to steel pins and no implant control. Representative (a) X-ray images (scale bar = 5 mm), (b) µCT images of femora over time in animals with steel or Mg2Ag implants compared to no implant control (scale bar = 2 mm), white arrow indicates degradation of the Mg2Ag pin, (c) µCT images of femoral midshaft cross sections at day 210 (scale bar = 0.5 mm), numbers indicate the width of the shaft diameter relative to no implant control ± SEM. N = 4 animals per group, $p \leq 0.05$, *significant compared to the group that received steel implants.

Fig. 4. (a) Quantification of body weight during 133 days after fracture fixation using an intramedullary Mg2Ag pin or a steel implant as control. Graph shows mean values ± SEM, n = 6-11 animals per group. (b) Representative images of hematoxylin & eosin-stained sections of liver, spleen, kidney and muscle at day 7 and day 133 after fracture and implantation of a Mg2Ag pin compared to mice that received a steel pin as control, 20x magnification (scale bar = 100µm), small boxes = area of digital magnification, large boxes: 13.5x digital zoom.

Fig. 5. Representative (a) X-ray images to determine implant positioning, callus formation and degradation of intramedullary Mg2Ag pins (scale bar = 5 mm), (b) µCT images of callus formation and fracture healing during 133 days in mice after fracture stabilization using a Mg2Ag implant compared to a steel pin as control (scale bar = 2 mm), (c) µCT images of cross sections of the femoral mid-shaft at day 133 post fracture (scale bar = 0.5 mm), numbers indicate the width of the shaft diameter relative to the control group that received steel implants ± SEM. N = 7-14 animals per group, $p \leq 0.05$, *significant compared to the group that received steel implants.

Fig. 6. (a) Representative images of mineralized bones on day 14, day 21 and day 133 after fracture stabilization using an intramedullary Mg2Ag pin or a steel implant, von Kossa/van Gieson staining (scale bar = 2 mm). (b) Quantification of the callus area, (c) relative amount of cartilage within the callus and (d) relative amount of mineralized bone within the callus during a time-course of 21 days after fracture stabilization using an intramedullary Mg2Ag pin or a steel implant. Graphs show mean ± SEM, n = 6-11 animals per group, $p \leq 0.05$, *significant compared to mice that received steel implants, $^{\#}$significant compared to day 7, $^{+}$significant compared to day 14.

Fig. 7. (a) Representative images of calcein/demeclocycline labeling at the periosteal elevation site on day 21 after fracture stabilization using an intramedullary Mg2Ag pin or a steel implant (scale bar = 20 µm). (b) Quantification of the periosteal mineral apposition rate (Ps MAR) at the same site on day 7, day 14 and day 21 after fracture stabilization. (c) Representative images of double labeling of trabecular bone surfaces within the callus by day 21 after fracture stabilization (scale bar = 20 µm). Quantification of (d) the bone formation rate / bone surface (BFR/BS), (e) the osteoid surface / bone surface (OS/BS), (f) the number of osteoblasts / bone surface (N.Ob/BS), (g) the eroded surface / bone surface (ES/BS), and (h) the number of osteoclasts / bone surface (N.Oc/BS) at the same site on day 21 after fracture stabilization using Mg2Ag pins or steel implants. Graphs show mean ± SEM, n = 6-11 animals per group, $p \leq 0.05$, *significant compared to the group that received steel implants.

References

[1] K.J. Agarwal-Harding, J.G. Meara, S.L.M. Greenberg, L.E. Hagander, D. Zurakowski, G.S.M. Dyer, Estimating the global incidence of femoral fracture from road traffic collisions: a literature review., J. Bone Joint Surg. Am. 97 (2015) e31.

[2] W.M. Ricci, B. Gallagher, G.J. Haidukewych, Intramedullary nailing of femoral shaft fractures: current concepts., J. Am. Acad. Orthop. Surg. 17 (2009) 296–305. http://www.ncbi.nlm.nih.gov/pubmed/19411641 (accessed December 9, 2015).

[3] T.A. Einhorn, & L.C. Gerstenfeld, Fracture healing: mechanisms and interventions, Nat. Rev. Rheumatol. (2015) 45–54.

[4] M.L. Busam, R.J. Esther, W.T. Obremskey, Hardware removal: indications and expectations., J. Am. Acad. Orthop. Surg. 14 (2006) 113–20. http://www.ncbi.nlm.nih.gov/pubmed/16467186 (accessed December 9, 2015).

[5] C. Krettek, C. Müller, R. Meller, M. Jagodzinski, F. Hildebrand, R. Gaulke, [Is routine implant removal after trauma surgery sensible?]., Unfallchirurg. 115 (2012) 315–22. d

[6] C. Krettek, P. Mommsen, [Implant removal after intramedullary osteosyntheses. Literature review, technical details, and tips and tricks]., Unfallchirurg. 115 (2012) 299–314.

[7] F. Witte, Reprint of: The history of biodegradable magnesium implants: A review, Acta Biomater. 23 (2015) S28–S40.

[8] A. Chaya, S. Yoshizawa, K. Verdelis, N. Myers, B.J. Costello, D.-T. Chou, et al., In vivo study of magnesium plate and screw degradation and bone fracture healing., Acta Biomater. 18 (2015) 262–9.

[9] A. Chaya, S. Yoshizawa, K. Verdelis, S. Noorani, B.J. Costello, C. Sfeir, Fracture healing using degradable magnesium fixation plates and screws., J. Oral Maxillofac. Surg. 73 (2015) 297, 299.

[10] M. Ezechieli, M. Ettinger, C. König, A. Weizbauer, P. Helmecke, R. Schavan, et al., Biomechanical characteristics of bioabsorbable magnesium-based (MgYREZr-alloy) interference screws with different threads, Knee Surgery, Sport. Traumatol. Arthrosc. (2014) 1–5.

[11] H.M. Wong, S. Wu, P.K. Chu, S.H. Cheng, K.D.K. Luk, K.M.C. Cheung, et al., Low-modulus Mg/PCL hybrid bone substitute for osteoporotic fracture fixation., Biomaterials. 34 (2013) 7016–32.

[12] H.M. Wong, Y. Zhao, V. Tam, S. Wu, P.K. Chu, Y. Zheng, et al., Invivo stimulation of bone formation by aluminum and oxygen plasma surface-modified magnesium implants, Biomaterials. 34 (2013) 9863–9876.

[13] F. Witte, V. Kaese, H. Haferkamp, E. Switzer, A. Meyer-Lindenberg, C.J. Wirth, et al., In vivo corrosion of four magnesium alloys and the associated bone response., Biomaterials. 26 (2005) 3557–63.

[14] T. Kraus, S.F. Fischerauer, A.C. Hänzi, P.J. Uggowitzer, J.F. Löffler, A.M. Weinberg, Magnesium alloys for temporary implants in osteosynthesis: in vivo studies of their degradation and interaction with bone., Acta Biomater. 8 (2012)

1230–8.

[15] S.Y. Cho, S.-W. Chae, K.W. Choi, H.K. Seok, Y.C. Kim, J.Y. Jung, et al., Biocompatibility and strength retention of biodegradable Mg-Ca-Zn alloy bone implants., J. Biomed. Mater. Res. B. Appl. Biomater. 101 (2013) 201–12.

[16] A. Krause, N. von der Höh, D. Bormann, C. Krause, F.-W. Bach, H. Windhagen, et al., Degradation behaviour and mechanical properties of magnesium implants in rabbit tibiae, J. Mater. Sci. 45 (2009) 624–632.

[17] J. Walker, S. Shadanbaz, T.B.F. Woodfield, M.P. Staiger, G.J. Dias, The in vitro and in vivo evaluation of the biocompatibility of Mg alloys., Biomed. Mater. 9 (2014) 015006.

[18] K. Pichler, T. Kraus, E. Martinelli, P. Sadoghi, G. Musumeci, P.J. Uggowitzer, et al., Cellular reactions to biodegradable magnesium alloys on human growth plate chondrocytes and osteoblasts., Int. Orthop. 38 (2014) 881–9.

[19] A. Burmester, B. Luthringer, R. Willumeit, F. Feyerabend, Comparison of the reaction of bone-derived cells to enhanced MgCl2-salt concentrations., Biomatter. 4 (2014) e967616.

[20] H. Windhagen, K. Radtke, A. Weizbauer, J. Diekmann, Y. Noll, U. Kreimeyer, et al., Biodegradable magnesium-based screw clinically equivalent to titanium screw in hallux valgus surgery: short term results of the first prospective, randomized, controlled clinical pilot study., Biomed. Eng. Online. 12 (2013) 62.

[21] Z. Li, X. Gu, S. Lou, Y. Zheng, The development of binary Mg-Ca alloys for use as biodegradable materials within bone., Biomaterials. 29 (2008) 1329–44. doi:10.1016/j.biomaterials.2007.12.021.

[22] M. Salahshoor, Y. Guo, Biodegradable Orthopedic Magnesium-Calcium (MgCa) Alloys, Processing, and Corrosion Performance, Materials (Basel). 5 (2012) 135–155.

[23] F. Witte, J. Fischer, J. Nellesen, C. Vogt, J. Vogt, T. Donath, et al., In vivo corrosion and corrosion protection of magnesium alloy LAE442., Acta Biomater. 6 (2010) 1792–9. doi:10.1016/j.actbio.2009.10.012.

[24] F. Feyerabend, J. Fischer, J. Holtz, F. Witte, R. Willumeit, H. Drücker, et al., Evaluation of short-term effects of rare earth and other elements used in magnesium alloys on primary cells and cell lines, Acta Biomater. 6 (2010) 1834–1842.

[25] D. Tie, F. Feyerabend, W.D. Müller, R. Schade, K. Liefeith, K.U. Kainer, et al., Antibacterial biodegradable Mg-Ag alloys., Eur. Cell. Mater. 25 (2013) 284–98; discussion 298. http://www.ncbi.nlm.nih.gov/pubmed/23771512 (accessed November 14, 2015).

[26] L. Wu, B.J.C. Luthringer, F. Feyerabend, A.F. Schilling, R. Willumeit, Effects of extracellular magnesium on the differentiation and function of human osteoclasts., Acta Biomater. 10 (2014) 2843–54.

[27] A. Bakker, J. Klein-Nulend, Osteoblast Isolation from Murine Calvariae and Long Bones, in: M.H. Helfrich, S.H. Ralston (Eds.), Bone Res. Protoc., 1st ed., Humana Press, 2003: pp. 19–28.

[28] N. Takahashi, N. Udagawa, S. Tanaka, T. Suda, Generating Murine

Osteoclasts from Bone Marrow, in: M.H. Helfrich, S.H. Ralston (Eds.), Bone Res. Protoc., 1st ed., Humana Press, 2003: pp. 129–144.

[29] E. Hesse, H. Saito, R. Kiviranta, D. Correa, K. Yamana, L. Neff, et al., Zfp521 controls bone mass by HDAC3-dependent attenuation of Runx2 activity, J. Cell Biol. 191 (2010) 1271–1283.

[30] D.W. Dempster, J.E. Compston, M.K. Drezner, F.H. Glorieux, J. a Kanis, H. Malluche, et al., Standardized nomenclature, symbols, and units for bone histomorphometry: a 2012 update of the report of the ASBMR Histomorphometry Nomenclature Committee., J. Bone Miner. Res. 28 (2013) 2–17.

[31] L. Wu, F. Feyerabend, A.F. Schilling, R. Willumeit-Römer, B.J.C. Luthringer, Effects of extracellular magnesium extract on the proliferation and differentiation of human osteoblasts and osteoclasts in coculture., Acta Biomater. 27 (2015) 294–304.

[32] A.H.M. Sanchez, B.J.C. Luthringer, F. Feyerabend, R. Willumeit, Mg and Mg alloys: How comparable are in vitro and in vivo corrosion rates? - A Review., Acta Biomater. (2014).

[33] A.C. Hänzi, I. Gerber, M. Schinhammer, J.F. Löffler, P.J. Uggowitzer, On the in vitro and in vivo degradation performance and biological response of new biodegradable Mg–Y–Zn alloys, Acta Biomater. 6 (2009) 1824–1833.

[34] C. Castellania, R.A. Lindtner, P. Hausbrandt, E. Tschegg, S.E. Stanzl-Tschegg, G. Zanoni, et al., Bone–implant interface strength and osseointegration: Biodegradable magnesium alloy versus standard titanium control, Acta Biomater. 7 (2010) 432–440.

[35] Z. Zhai, X. Qu, H. Li, K. Yang, P. Wan, L. Tan, et al., The effect of metallic magnesium degradation products on osteoclast-induced osteolysis and attenuation of NF-κB and NFATc1 signaling, Biomaterials. 35 (2014) 6299–6310.

[36] Z. Chen, X. Mao, L. Tan, T. Friis, C. Wu, R. Crawford, et al., Osteoimmunomodulatory properties of magnesium scaffolds coated with β-tricalcium phosphate, Biomaterials. 35 (2014) 8553–8565.

[37] C. Rössig, N. Angrisani, P. Helmecke, S. Besdo, J.-M. Seitz, B. Welke, et al., In vivo evaluation of a magnesium-based degradable intramedullary nailing system in a sheep model., Acta Biomater. 25 (2015) 369–83.

Figure 1:

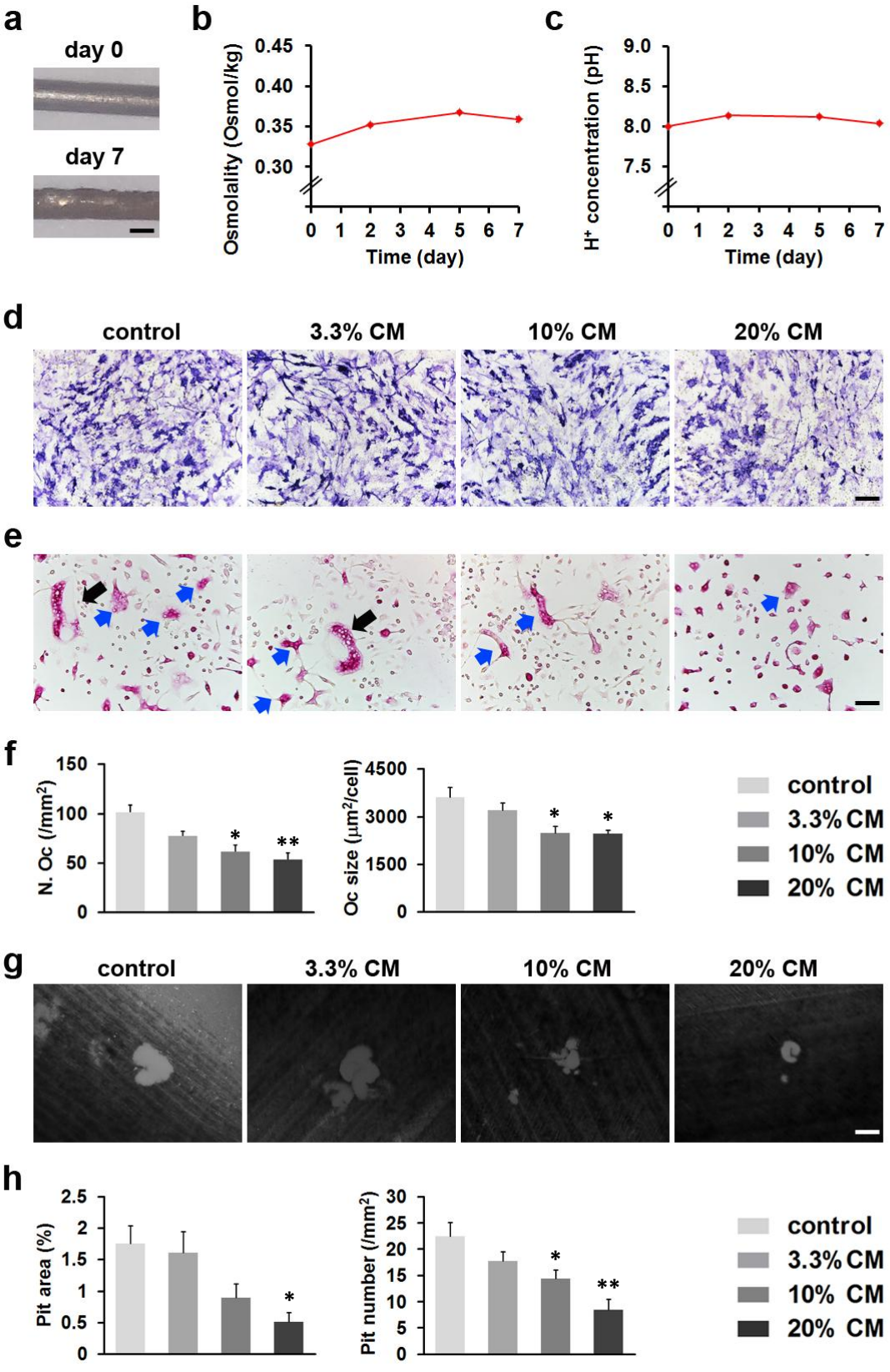
a
day 0
day 7
b
Osmolality (Osmol/kg)
0.45
0.40
0.35
0.30
0 1 2 3 4 5 6 7
Time (day)
c
H+ concentration (pH)
9.0
8.5
8.0
7.5
0 1 2 3 4 5 6 7
Time (day)
d
control
3.3% CM
10% CM
20% CM
e
f
N. Oc (/mm2)
150
100
50
0
*
**
Oc size (μm2/cell)
4500
3000
1500
0
*
*
control
3.3% CM
10% CM
20% CM
g
control
3.3% CM
10% CM
20% CM
h
Pit area (%)
2.5
2
1.5
1
0.5
0
*
Pit number (/mm2)
30
25
20
15
10
5
0
*
**
control
3.3% CM
10% CM
20% CM

Figure 2:

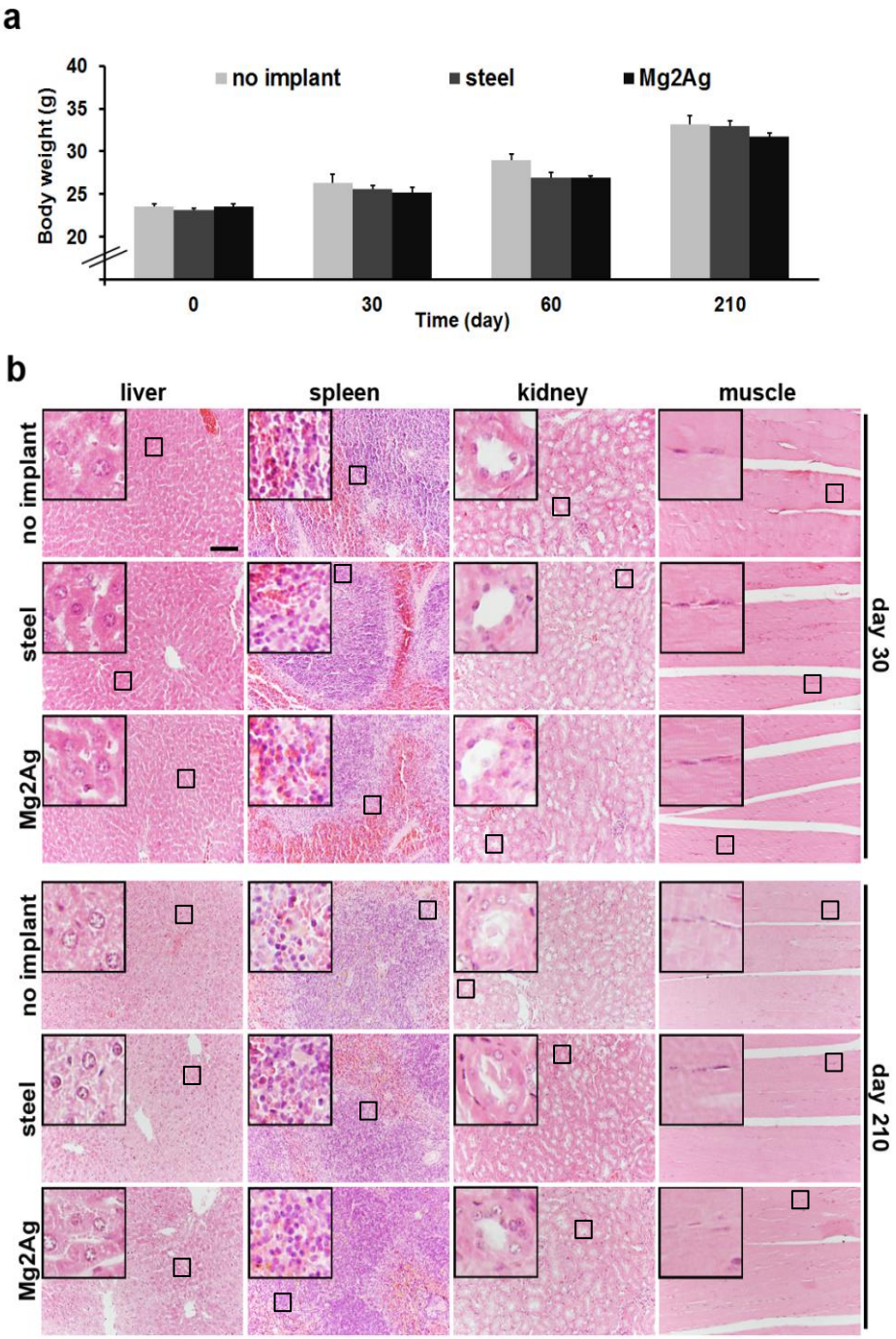
a
no implant
steel
Mg2Ag
Body weight (g)
40
35
30
25
20
0
30
60
210
Time (day)
b
liver
spleen
kidney
muscle
no implant
steel
Mg2Ag
day 30
day 210

Figure 3:

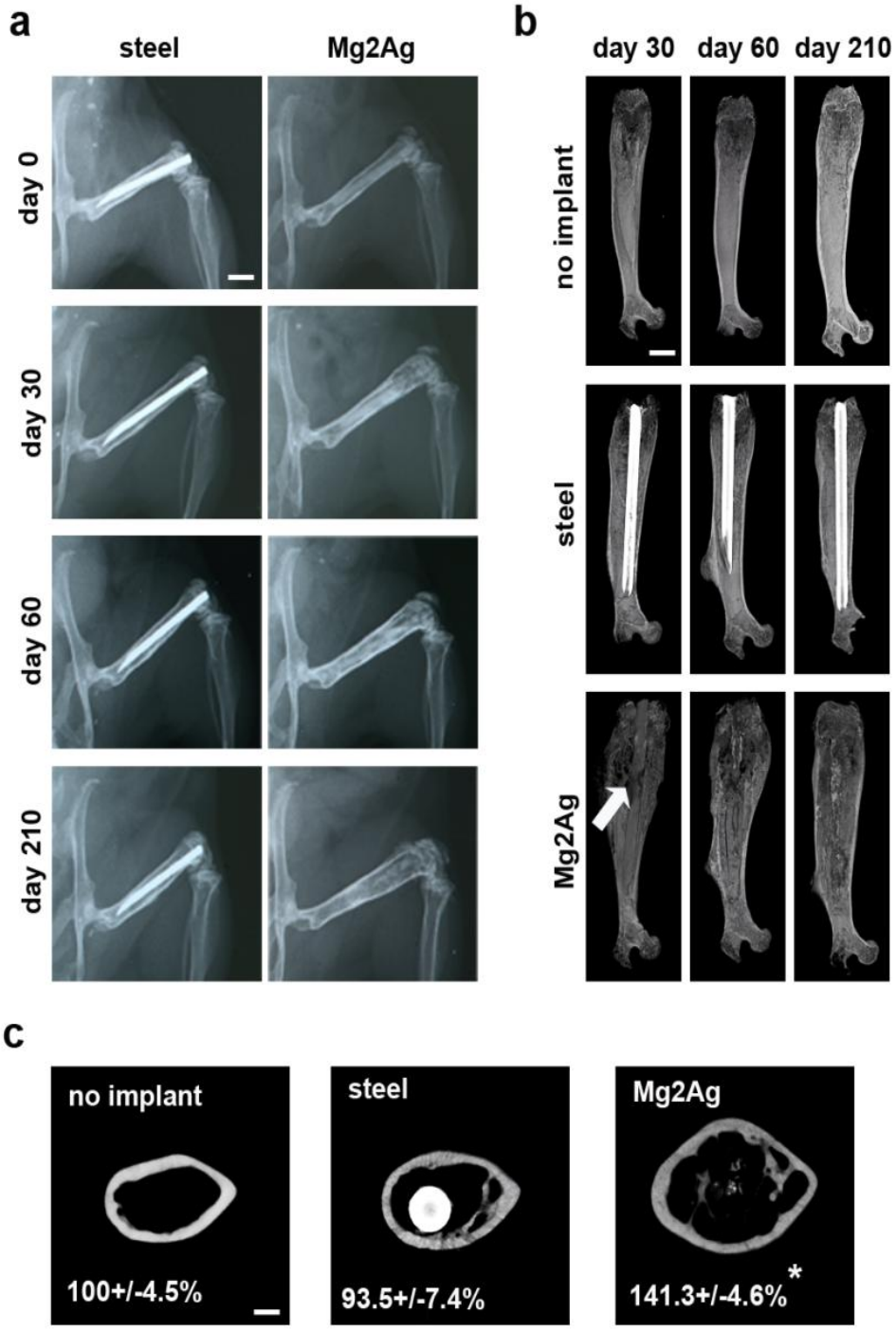
a
steel
Mg2Ag
day 0
day 30
day 60
day 210
b
day 30
day 60
day 210
no implant
steel
Mg2Ag
c
no implant
100+/-4.5%
steel
93.5+/-7.4%
Mg2Ag
141.3+/-4.6%*

Figure 4:

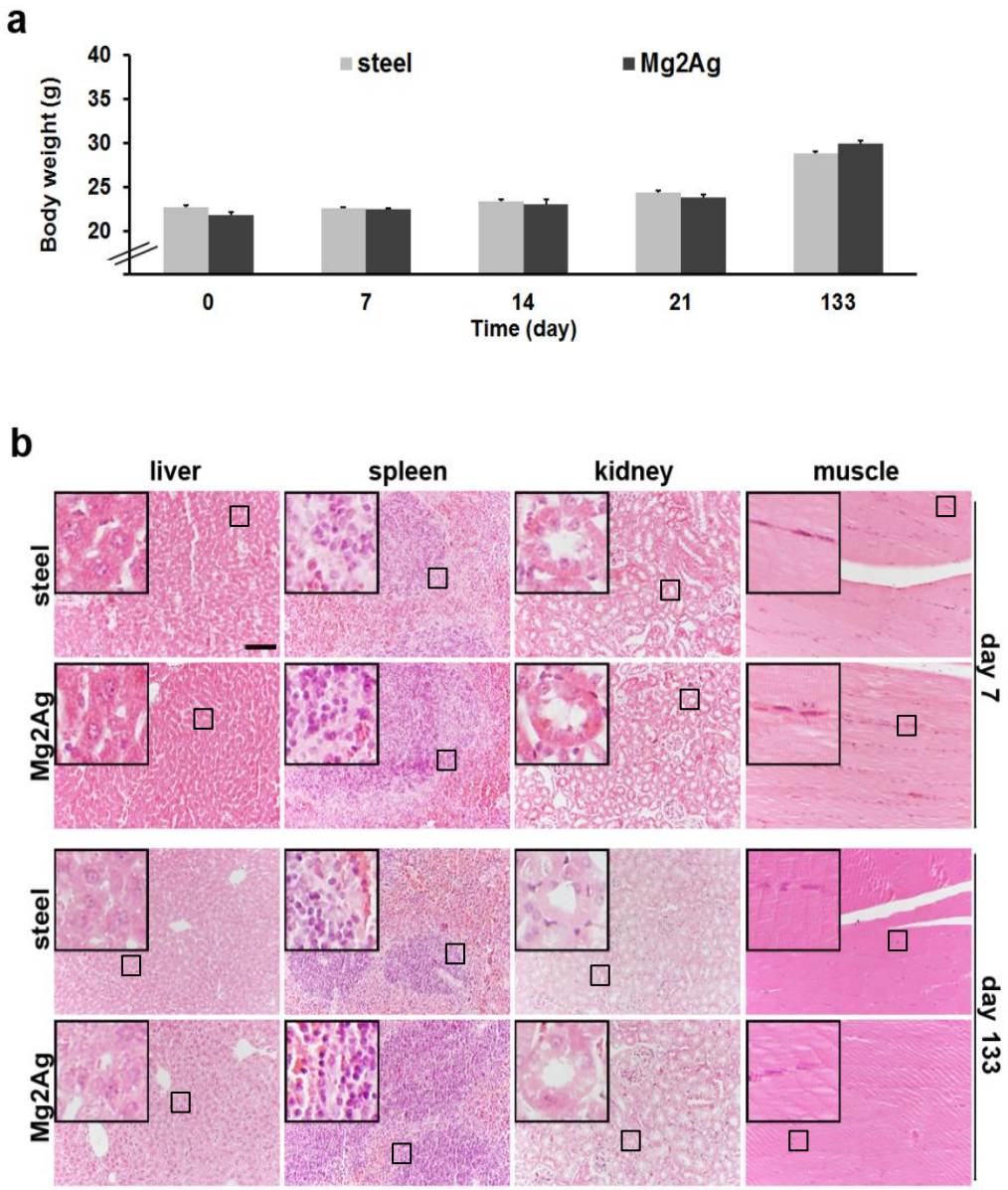
a
steel
Mg2Ag
Body weight (g)
40
35
30
25
20
0
7
14
21
133
Time (day)
b
liver
spleen
kidney
muscle
steel
Mg2Ag
day 7
steel
Mg2Ag
day 133

Figure 5:

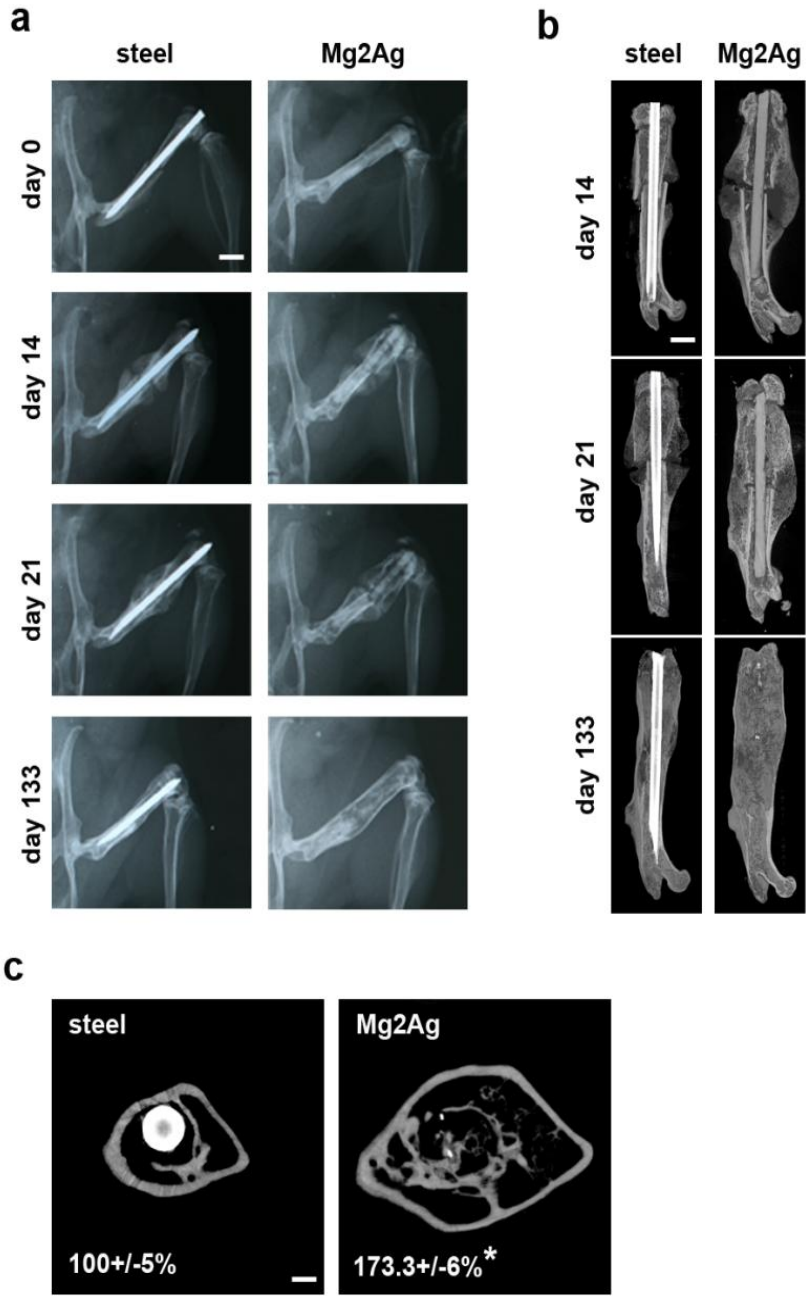
a
steel
Mg2Ag
day 0
day 14
day 21
day 133
b
steel
Mg2Ag
day 14
day 21
day 133
c
steel
Mg2Ag
100+/-5%
173.3+/-6%*

Figure 6:

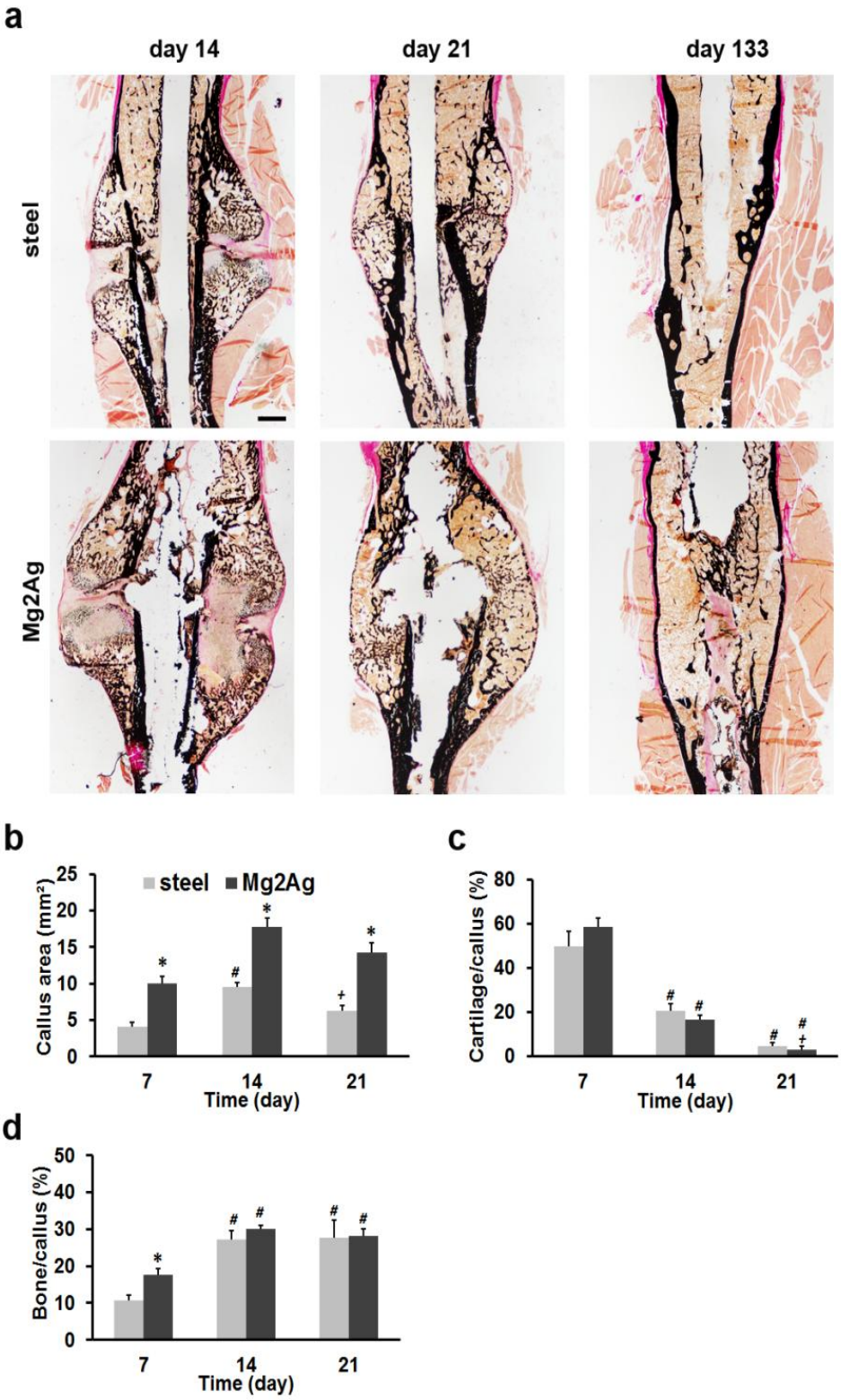
a
day 14
day 21
day 133
steel
Mg2Ag
b
steel
Mg2Ag
Callus area (mm²)
Time (day)
c
Cartilage/callus (%)
Time (day)
d
Bone/callus (%)
Time (day)

Figure 7:

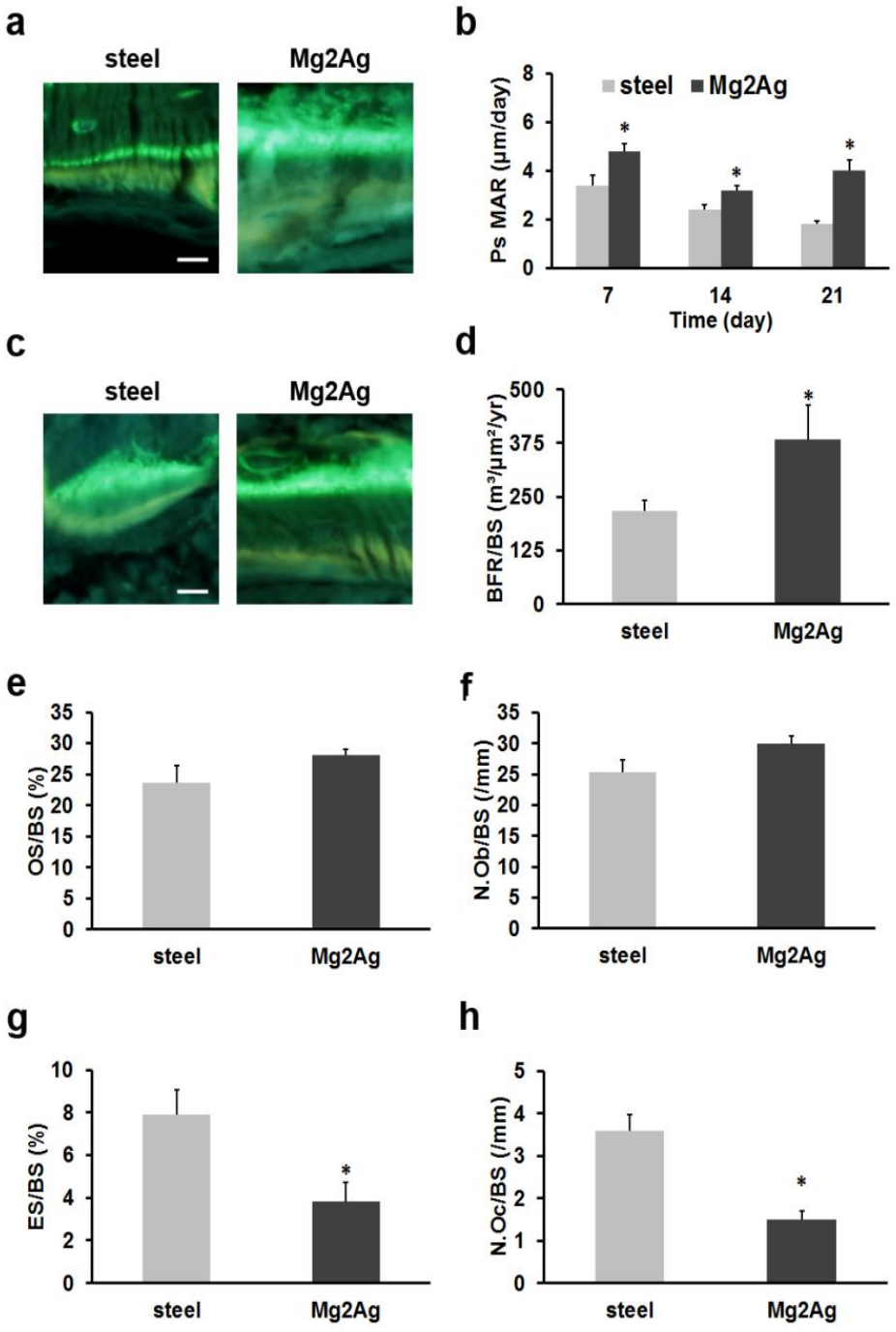
a
steel
Mg2Ag
b
steel
Mg2Ag
Ps MAR (μm/day)
0
2
4
6
8
*
*
*
7
14
21
Time (day)
c
steel
Mg2Ag
d
BFR/BS (m³/μm²/yr)
0
125
250
375
500
*
steel
Mg2Ag
e
OS/BS (%)
0
5
10
15
20
25
30
35
steel
Mg2Ag
f
N.Ob/BS (/mm)
0
5
10
15
20
25
30
35
steel
Mg2Ag
g
ES/BS (%)
0
2
4
6
8
10
*
steel
Mg2Ag
h
N.Oc/BS (/mm)
0
1
2
3
4
5
*
steel
Mg2Ag

*Graphical Abstract

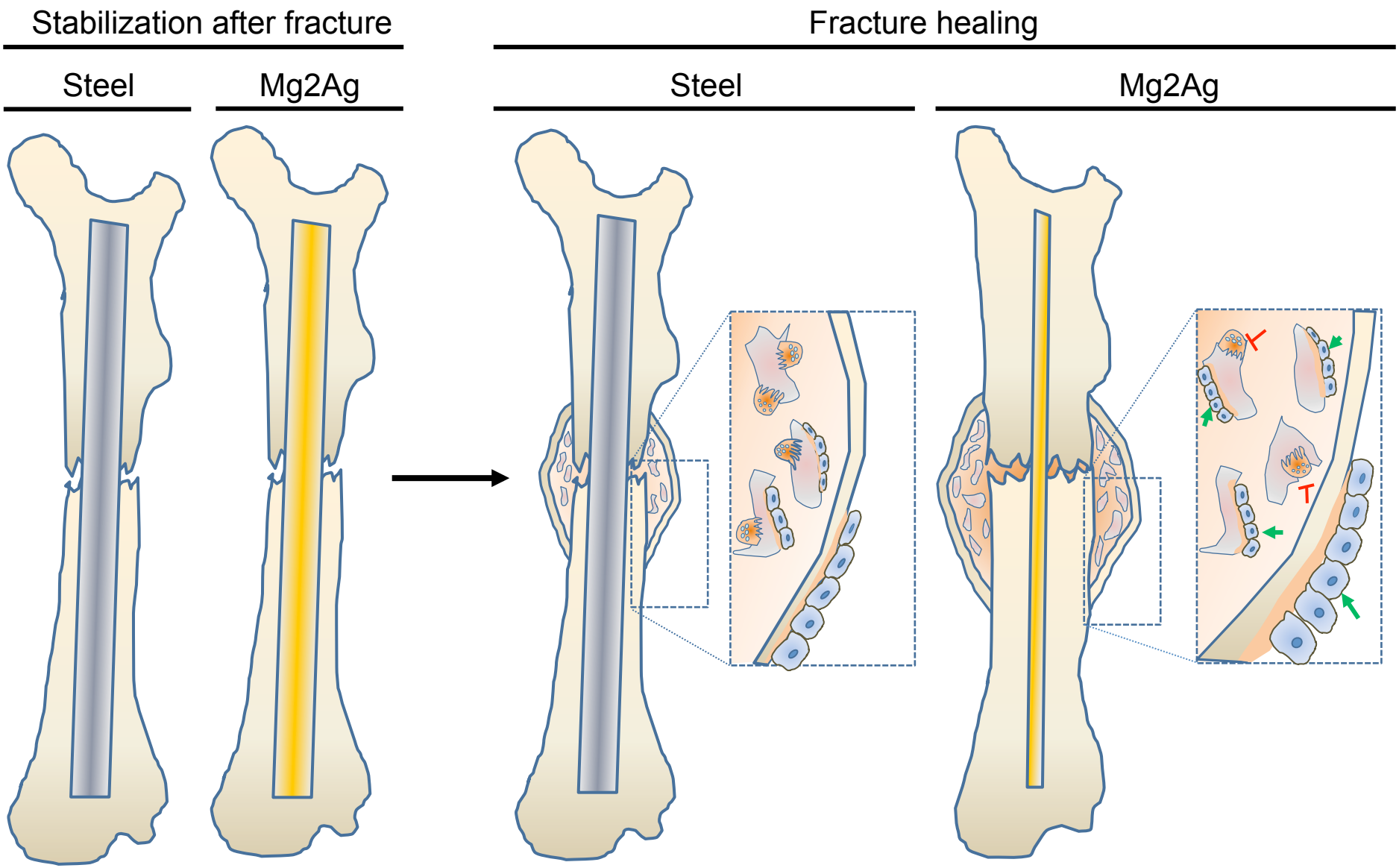

Statement of Significance

Biodegradable implants are promising alternatives to standard steel or titanium implants to avoid implant removal after fracture healing. We therefore developed an intramedullary nail using a novel biodegradable magnesium-silver-alloy (Mg2Ag) and investigated the *in vitro* and *in vivo* effects of the implants on bone remodeling under steady state and fracture healing conditions in mice. Our results demonstrate that intramedullary Mg2Ag nails degrade *in vivo* over time without causing adverse effects. Importantly, radiographs, µCT and bone histomorphometry revealed a significant increase in callus size due to an augmented bone formation rate and a reduced bone resorption in fractures supported by Mg2Ag nails, thereby improving bone healing. Thus, intramedullary Mg2Ag nails are promising biomaterials for fracture healing to circumvent implant removal.